Structure
Article

Accessory Proteins Stabilize the Acceptor Complex for Synaptobrevin, the 1:1 Syntaxin/SNAP-25 Complex

Keith Weninger,[1,5] Mark E. Bowen,[2,5] Ucheor B. Choi,[1] Steven Chu,[3] and Axel T. Brunger[4,*]
[1]Department of Physics, North Carolina State University, Raleigh, NC 27695-8202, USA
[2]Department of Physiology and Biophysics, Stony Brook University Medical Center, Stony Brook, NY 11794-8661, USA
[3]Lawrence Berkeley National Laboratory, Berkeley, CA 94720, USA
[4]Howard Hughes Medical Institute and Departments of Molecular and Cellular Physiology, Neurology and Neurological Sciences, Structural Biology, and Photon Science, Stanford University, Stanford, CA 94305, USA
[5]These authors contributed equally to this work.
*Correspondence: brunger@stanford.edu
DOI 10.1016/j.str.2007.12.010

SUMMARY

Syntaxin/SNAP-25 interactions precede assembly of the ternary SNARE complex that is essential for neurotransmitter release. This binary complex has been difficult to characterize by bulk methods because of the prevalence of a 2:1 dead-end species. Here, using single-molecule fluorescence, we find the structure of the 1:1 syntaxin/SNAP-25 binary complex is variable, with states changing on the second timescale. One state corresponds to a parallel three-helix bundle, whereas other states show one of the SNAP-25 SNARE domains dissociated. Adding synaptobrevin suppresses the dissociated helix states. Remarkably, upon addition of complexin, Munc13, Munc18, or synaptotagmin, a similar effect is observed. Thus, the 1:1 binary complex is a dynamic acceptor for synaptobrevin binding, and accessory proteins stabilize this acceptor. In the cellular environment the binary complex is actively maintained in a configuration where it can rapidly interact with synaptobrevin, so formation is not likely a limiting step for neurotransmitter release.

INTRODUCTION

Neurotransmitter release depends on the Ca^{2+}-dependent fusion of synaptic vesicles with the presynaptic plasma membrane (Stevens, 2003; Südhof, 2004). This highly regulated process is governed at all levels, from vesicle formation to targeting and fusion, by a series of sequential protein/protein interactions (Südhof, 2004; Brunger, 2005; Jackson and Chapman, 2006; Jahn and Scheller, 2006). The SNARE (soluble N-ethylmaleimide-sensitive factor attachment protein receptor) family of proteins is essential for the final stages of synaptic vesicle fusion (Duman and Forte, 2003; Kidokoro, 2003). At the synapse, three SNARE proteins, syntaxin and SNAP-25 (synaptosome-associated protein of 25 kDa) on the plasma membrane and synaptobrevin on synaptic vesicles, form a heterotrimeric SNARE complex that bridges the vesicle and plasma membrane (Söllner et al., 1993). The neuronal SNARE complex is sufficient to dock lipid vesicles and promote lipid mixing in vitro (Weber et al., 1998), although the extent and kinetics of lipid mixing and fusion are highly dependent on the experimental conditions (Bowen et al., 2004; Fix et al., 2004; Liu et al., 2005; Pobbati et al., 2006). In addition, the transmembrane domains of synaptobrevin and particularly syntaxin disrupt membranes and favor fusion pore opening (Dennison et al., 2006). Although the molecular mechanism by which SNAREs participate in Ca^{2+}-triggered synaptic vesicle fusion is still uncertain (Duman and Forte, 2003; Rizo et al., 2006), SNAREs must play a key role in the process, as disruption of SNARE complex formation by knockout (Schoch et al., 2001) or separation of the complex from the transmembrane domains by clostridial neurotoxins inhibits neurotransmitter release (Humeau et al., 2000).

The pathway for SNARE complex assembly in vivo remains unclear. SNARE interactions in vitro are promiscuous, resulting in low specificity for cognate binding partners (Fasshauer et al., 1999), whereas mixtures of alternate configurations form during assembly in solution (Weninger et al., 2003). As SNARE domains are largely unstructured as monomers, complex formation is coupled to protein folding of SNAREs (Fasshauer et al., 1997a, 1997b; Fiebig et al., 1999).

Assembly of the heterotrimeric SNARE complex is thought to begin with a binary "acceptor" complex between syntaxin and SNAP-25 with 1:1 stoichiometry (Fasshauer and Margittai, 2004), although other binary SNARE interactions have also been observed (Woodbury and Rognlien, 2000; Chen et al., 2001; Bowen et al., 2004; Liu et al., 2006). Syntaxin and SNAP-25 can also form a 2:1 species in vitro where an additional syntaxin molecule occupies the binding site for synaptobrevin in the ternary SNARE complex (Margittai et al., 2001; Xiao et al., 2001). Although less stable than the ternary SNARE complex, the 2:1 species of the syntaxin/SNAP-25 complex dissociates slowly (Fasshauer and Margittai, 2004), so it represents a kinetically trapped dead-end state that would require chaperones for disassembly in vivo. Furthermore, prevention of formation of the 2:1 species greatly accelerates the lipid mixing observed in liposome assays in vitro (Pobbati et al., 2006). Finally, the 2:1 species is not conserved, for example it does not occur with the yeast sso1/sec9 t-SNARE complex (Nicholson et al., 1998; Fiebig et al., 1999). FRET studies in PC12 cells (An and Almers, 2004) indicated that, in vivo, the syntaxin/SNAP-25 complex is fundamentally different from the ternary SNARE complex (Sutton et al., 1998; Ernst and Brunger, 2003) and from the 2:1 species

(Margittai et al., 2001; Xiao et al., 2001; Zhang et al., 2002), but the bulk character of the study prevented a more detailed structural interpretation. Taken together, the 2:1 species of the syntaxin/SNAP-25 complex is likely not a physiological intermediate on the pathway to vesicle fusion.

The tendency to form the 2:1 species at high protein concentration has precluded the study of the 1:1 binary complex by structural methods such as X-ray crystallography or nuclear magnetic or electron paramagnetic resonance spectroscopy. Here we used single-molecule fluorescence resonance energy transfer (smFRET) to characterize the binary complex under conditions that favor the 1:1 species. Binary complexes were formed in supported bilayers containing full-length syntaxin at extremely low protein-to-lipid ratios. The low protein concentration along with the limited mobility of syntaxin in the bilayer maximizes formation of the 1:1 complex. Inter- and intramolecular smFRET efficiency was measured between a series of labeling site pairs in syntaxin and SNAP-25. The dissociation rate of the 1:1 binary complex is slow, but the complex showed substantial conformational variability. These conformations could be rapidly locked into a single FRET efficiency state by the addition of synaptobrevin. Thus, the 1:1 syntaxin/SNAP-25 complex serves as a dynamic acceptor for synaptobrevin binding. We also studied the effect of adding complexin, Munc13, Munc18, or synaptotagmin to the binary complex. Surprisingly, we found that all of these proteins, but not bovine serum albumin (BSA) or buffer-only controls, lock the binary complex into a single configuration.

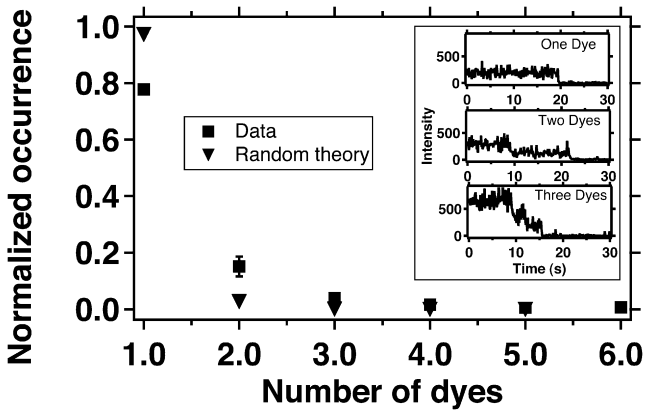

Figure 1. Syntaxin Monodispersity in Supported Lipid Bilayers

Acceptor-labeled syntaxin was reconstituted into supported lipid bilayers at concentrations that were low enough to spatially resolve individual molecules (73 ± 30 labeled protein molecules in the view area of 45 × 90 μm, obtained from a protein-to-lipid ratio of $1{:}10^7$ during reconstitution). Individual photobleaching steps were counted in intensity time traces from observed spots to assess the aggregation state. Examples of one, two, and three dyes are shown in the inset. The normalized frequency of occurrence is plotted as a histogram. The error bars represent variability in separate trials using alternate labeling sites, different fluorescent dyes, as well as with and without Ca^{2+} and EDTA. Also shown is the theoretical frequency of occurrence of molecules being colocalized in observed spots assuming a random distribution of molecules (see Experimental Procedures for details).

RESULTS

To investigate the conformation of the binary complex and the folding pathway that leads to SNARE complex formation, we designed a series of SNARE constructs with specific mutations for labeling with fluorescent dyes and studied their interactions by smFRET. Multiple dye combinations and labeling sites were used to limit the possibility of the dyes influencing the results.

The cytoplasmic domain of syntaxin dimerizes with micromolar affinity and forms tetramers with ten micromolar to millimolar affinity (Lerman et al., 2000). In addition, the syntaxin transmembrane domain has a tendency to weakly self-associate (Laage et al., 2000; Bowen et al., 2002; Kroch and Fleming, 2006). In order to maximize formation of the 1:1 syntaxin/SNAP-25 complex, we sought to isolate syntaxin monomers in a supported bilayer by reconstituting syntaxin at very low protein-to-lipid ratios ($1{:}10^6$ or $1{:}10^7$). Using conservative assumptions in the analysis (Figure 1; Experimental Procedures), at least 50% of the syntaxin molecules are monomeric and will therefore form 1:1 complexes upon addition of SNAP-25. The actual number of 1:1 complexes is likely higher, as discussed below.

Binary Complex Formation and Stability

We first tested binding of labeled SNAP-25 to several different surfaces. SNAP-25 showed very little nonspecific binding to protein-free bilayers (Figure 2A, first triangle and first circle; Figure 2B, squares). Nonspecific binding of SNAP-25 to lipid bilayers was not found to depend strongly on length of exposure for times ranging from 15 min to 24 hr. When unlabeled syntaxin was incorporated into the egg phosphatidylcholine (PC) bilayer, we observed increasing levels of SNAP-25 recruitment to the bilayer that scaled with the syntaxin concentration. SNAP-25 has been reported to bind to syntaxin with an on-rate of 6000 $M^{-1}s^{-1}$ (Fasshauer and Margittai, 2004). Based upon the low concentration of SNAP-25 (60 nM), the characteristic time of the binding reaction in our experiment is expected to be around 280 min. Considering a 20 min waiting period prior to the start of the illumination, we estimate that the reaction should have proceeded to about $\sim$1-$e^{-20/280}$, or only 7% saturation. This estimate agrees well with the extent of binding that we observe at concentrations of 1–10 syntaxin/μm^2 (Figure 2A), particularly when considering that our reconstitution method orients about half of the syntaxins in the bilayer toward the optical surface.

Studies in PC12 cells had suggested that SNAP-25 binding to synaptobrevin might be the first step in SNARE complex formation (Chen et al., 2001), although other studies do not support formation of a stable synaptobrevin/SNAP-25 binary complex (Lang et al., 2002; An and Almers, 2004). The synaptobrevin/SNAP-25 interaction is the weakest among all pairwise SNARE domain interactions as assessed by circular dichroism experiments (Fasshauer et al., 1998a), but it can be observed by GST pull-down experiments (Chapman et al., 1994). The dissociation constant between synaptobrevin and SNAP-25 is K_D = 1–1.4 μM (depending on which protein is GST tagged in the pull-down experiment), compared to that between syntaxin and SNAP-25, K_D = 0.4 μM (using GST-syntaxin for the pull-down) (Pevsner et al., 1994). Likewise, there is a weak interaction between synaptobrevin and SNAP-23 (Foster et al., 1998). To test whether this interaction can be observed with single-molecule microscopy experiments, we incubated SNAP-25 above supported bilayers containing unlabeled full-length synaptobrevin. SNAP-25 binding was also

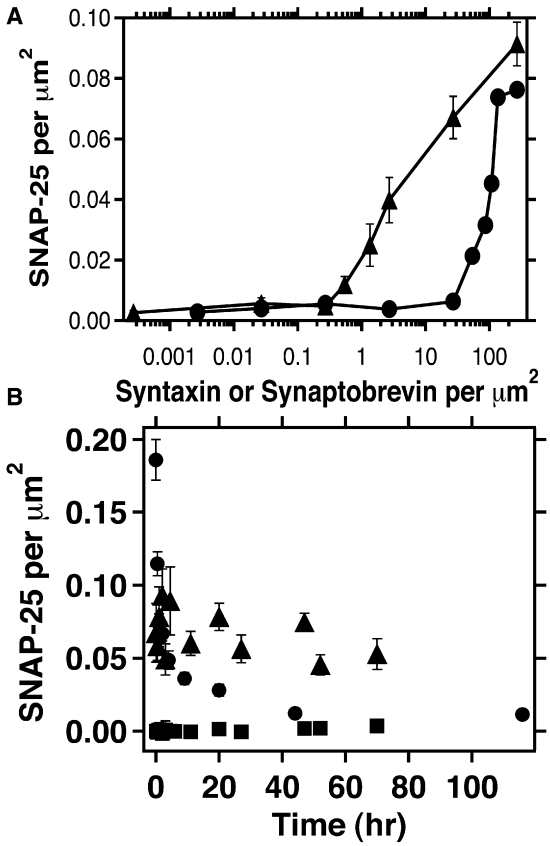

Figure 2. Binary SNARE Complex Interactions on Supported Lipid Bilayers

(A) SNAP-25 N139C (Cy3) was incubated at room temperature above protein-containing, supported lipid bilayers at 60 nM for 20 min and rinsed away. Unlabeled syntaxin (triangles) or unlabeled synaptobrevin (circles) was present in the supported bilayer at the concentrations indicated in the abscissa. The first point for each curve represents protein-free bilayer. For each condition, the surface concentration of SNAP-25 molecules retained at the bilayers was sampled at many (>10) locations and averaged to yield a point on the graph. The full width of the error bars reports two times the standard deviation accompanying that average. These data report one experiment, but the results were independently reproduced three times.

(B) Cy3-SNAP-25-labeled binary complexes were assembled on bilayers containing 50–100 protein molecules/μm^2 (triangles for syntaxin and circles for synaptobrevin) as in (A), after which excess SNAP-25 was rinsed away. The bilayers were then stored in a 37°C incubator and removed periodically to allow SNAP-25 surface density to be measured at room temperature with the single-molecule microscope to assess the spontaneous disassembly of the binary complexes. Bilayers were returned to 37°C following each periodic count. The squares represent a control using a protein-free lipid bilayer that received the same SNAP-25 incubation. Error bars indicate the standard deviation of the average of ten randomly sampled locations on the bilayers.

observed, albeit at nearly 100-fold higher protein concentration compared to syntaxin bilayers (Figure 2A, circles).

Once binary complexes between syntaxin and SNAP-25 were assembled on supported bilayers, they were very stable with little spontaneous disassembly detected over long timescales (Figure 2B, triangles). The observed high stability of the syntaxin/SNAP-25 binary complex agrees with other studies using changes in fluorescence anisotropy upon competitive dissociation (Pobbati et al., 2006) and extrapolation of GdnHCl unfolding experiments (Fasshauer et al., 2002). In contrast, we observed faster spontaneous disassembly of the synaptobrevin/SNAP-25 complex (Figure 2B, circles), indicating a greater off-rate for this weaker complex.

Configurations of the 1:1 Binary Complex: Labels on Syntaxin and SNAP-25

We next investigated the configurations of the 1:1 syntaxin/SNAP-25 complex using smFRET. SNAP-25 was labeled with the donor dye near the N terminus (Q20C) of its first SNARE domain (SN1), and full-length syntaxin was labeled with an acceptor dye at the N terminus of its SNARE domain (S193C). In the ternary SNARE complex, this particular labeling site pair produces two populations, the majority population exhibiting full FRET (indicating a parallel configuration between syntaxin and SN1) and a smaller population with FRET = 0 (indicating an antiparallel configuration) with no significant intermediate FRET population (Weninger et al., 2003). Because these site pairs showed high FRET in the SNARE complex, we used the appearance of non-zero FRET within the first second of the observation period to select complexes for further analysis. Binary complexes were formed in situ on syntaxin containing supported bilayers at a protein-to-lipid ratio of $1:10^7$. The probability of observing a given FRET efficiency state in the binary complex is shown in Figure 3A, and representative time traces are shown in Figure 3C.

We observed high and low FRET efficiency states for the binary complex similar to that seen in the ternary complex (Weninger et al., 2003). However, we also observed a large number of intermediate FRET efficiency states that were not observed in the ternary SNARE complex. Theses intermediate states cover the entire range of possible FRET efficiency values, so they cannot represent a single intermediate conformation. Examination of individual fluorescence intensity time traces showed a wide variety of dynamic behaviors (Figure 3C). We observed complexes that switched between low FRET (donor high while acceptor is low) and high FRET (acceptor high while donor is low) on timescales of 0.1–1 s (top panel), whereas others displayed more stable intermediate FRET efficiency states (donor and acceptor at a similar level, middle and bottom panels). Fifteen percent of the complexes in this experiment switched states at least once during the 45 s observation period. The intermediate levels and dynamic changes of FRET efficiency values suggest that the binary complex samples a variety of configurations rather than adopting a unique structure. The transitions between FRET efficiency states imply that the dye attachment sites are moving more than 5 nm. Thus, in the binary complex, the SNARE domains can adopt configurations very different from that of the ternary SNARE complex.

Addition of the cytoplasmic domain of synaptobrevin (residues 1–96) to the binary complex eliminated the intermediate FRET states and dynamic behavior (Figures 3B and 3D). Only the high and low FRET populations characteristic of the ternary SNARE complex remained (Weninger et al., 2003). No state switching or stable intermediate FRET efficiency states were observed in any of the corresponding time traces following synaptobrevin exposure (Figure 3D).

Time traces for the binary and ternary SNARE complexes were obtained under identical buffer, labeling, and illumination conditions. Thus, the dynamic behavior observed in the binary

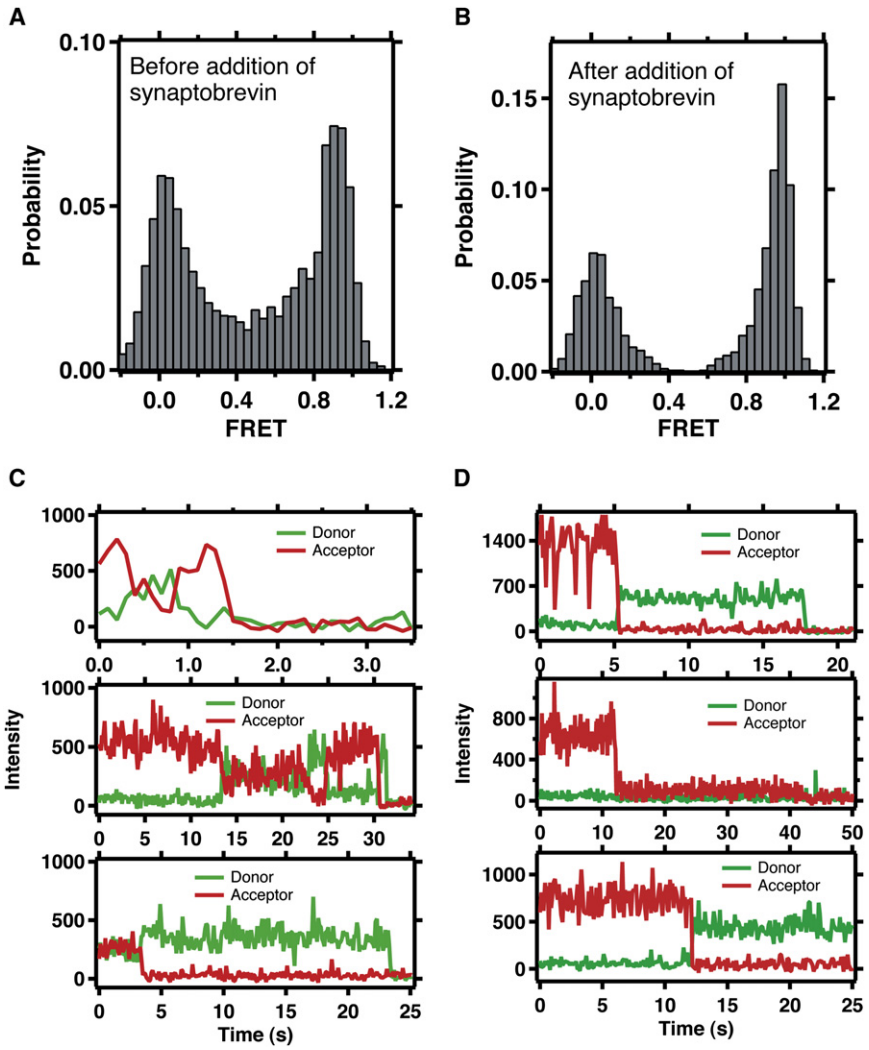

Figure 3. smFRET Measurements of Binary Syntaxin/SNAP-25 Complexes with Dyes Attached to Syntaxin and SN1, and the Effect of the Addition of Synaptobrevin

Lipid bilayers were formed with acceptor-labeled syntaxin (S193C-Cy5) sufficiently diluted to allow imaging of individual proteins similar to the conditions of Figure 1. All experiments were collected under identical buffer and illumination conditions. In (A), donor-labeled SNAP-25 (Q20C-Cy3) was incubated at 75 nM for 18 hr over the syntaxin bilayer and then rinsed away. FRET efficiency values for individual binary complexes that exhibited nonzero FRET within the first half-second of illumination were calculated frame by frame and compiled into a histogram. As such, the histograms represent the probability of a binary complex exhibiting a particular FRET efficiency level rather than the number of complexes observed at a given FRET level. In (B), inclusion of 125 nM synaptobrevin (residues 1–96) during the 18 hr incubation of 75 nM SNAP-25 over syntaxin bilayers eliminated the population with intermediate FRET. Representative time traces are shown in (C) and (D). All time traces were obtained with green illumination. Green laser illumination does not give rise to acceptor emission, so acceptor emission indicates FRET due to close proximity of the donor dye. Eventual photobleaching events are visible for all but one dye ([D], bottom trace). (C) shows representative individual time traces for binary SNARE complexes corresponding to the experiments summarized in (A). Note the stochastic switching of FRET efficiency values as well as sustained intermediate FRET for some of the traces, which can be interpreted as switching between high and low FRET on timescales faster than the 0.1 s temporal resolution of the measurement. (D) shows representative individual time traces after synaptobrevin was added to the binary complex (corresponding to the experiments summarized in [B]). Intermediate FRET efficiency states and dynamic changes in FRET efficiency are absent. The observed single steps correspond to photobleaching of the acceptor (upper and lower panels) or the donor (middle panel).

complex is the result of conformational differences and cannot be the result of dye photophysics such as blinking.

Doubly Labeled SNAP-25

To further characterize the structure of the binary complex, we created combinations of donor/acceptor labeling site pairs on SNAP-25 itself within its two SNARE domains (SN1 and SN2): C terminus of SN1 versus C terminus of SN2 (CC); N terminus of SN1 versus C terminus of SN2 (NC); and N terminus of SN1 versus N terminus of SN2 (NN). These double mutants allowed examination of the relative configuration of the two SNARE domains in SNAP-25. Doubly labeled proteins were prepared by simultaneous reaction with two dyes such that either labeling site could contain either the donor or acceptor dye. Labeling efficiency was high at both sites (>80%), and the protein samples were monomeric as assessed by gel filtration (data not shown). An alternating red and green laser illumination scheme allowed us to select for analysis molecules with exactly one donor and one acceptor dye.

We formed complexes between the doubly labeled SNAP-25 mutants and unlabeled syntaxin reconstituted into supported egg PC bilayers. Because of the high labeling efficiency and monodispersity of SNAP-25, all single dye pairs could be reliably assumed to correspond to exactly one SNAP-25 molecule. We confirmed this expectation by labeling a sample of SNAP-25 NC with only donor dye and a second sample of SNAP-25 NC with only acceptor dye. We then made an equimolar mixture of these two samples that we introduced above, a syntaxin containing bilayer to form binary complexes. Our red-green alternating laser illumination allowed us to diagnose the population of binary complexes that contained at least one of each different dye species. Sampling over 1000 binary complexes, we found that about 4% of acceptor containing observation spots also had a donor present. When we required that FRET be present

between the donor and acceptor, a stricter criterion that will eliminate some of the unavoidable occurrences of two SNAP-25 molecules that are not complexed together but that randomly reside within a distance smaller than the optical resolution of our instrument, we found that only 0.4% of colocalized complexes contain two SNAP-25 molecules with donor and acceptor dyes positioned within the range of FRET. We conclude that complexes of one syntaxin and two SNAP-25 molecules occur less than one-half-percent of the time. We therefore returned to using SNAP-25 complexes labeled with mixtures of donor and acceptor dye in order to use FRET to characterize the binary 1:1 complex.

Figures 4A, 4C, and 4E show the FRET efficiency distributions for binary complexes formed from the NN, CC, and NC SNAP-25 constructs, respectively. In all cases, populations of low, intermediate, and high FRET efficiency states were observed. Note that we observed a more pronounced intermediate FRET = 0.5 state for these labeling combinations compared to the SNAP-25/syntaxin labeling combination (Figure 3A). In the cases with dye labels positioned to report a parallel configuration, NN and CC (Figures 4A and 4C), we find large populations in a high FRET state. Thus, the binary complex preferentially assembles with the SN1 and SN2 SNARE domains oriented in a parallel configuration similar to their orientation in the ternary SNARE complex. The NC labeling combination (Figure 4C), for which the labels would be separated by more than 8 nm if it were in the parallel configuration of the ternary SNARE complex, showed a pronounced intermediate FRET efficiency state (near FRET = 0.5). These observations are consistent with a model wherein SN1 and SN2 maintain a predominantly parallel orientation with each other as in the ternary complex. However, as was observed for the syntaxin/SNAP-25 labeling combinations, there is significant conformational variability in the binary complex that allows the termini to get closer (within 5 nm) than in the extended helical bundle of the ternary complex. The fluorescence intensity time traces for the doubly labeled SNAP-25 binary complex showed stable intermediate FRET, stable high FRET, and dynamic switching between otherwise stable states similar to the data in Figure 3C (see Figure S2 in the Supplemental Data available with this article online). Averaging over four independent experiments, we found that 10.7% of complexes (standard error of the mean 2.3%) exhibited at least one switch between mid and high FRET states during the ~1 min observation window.

Next, we added the unlabeled synaptobrevin cytosolic domain above the supported bilayer for 90 min to form the ternary SNARE complex in situ (Figures 4B, 4D, and 4F). Similar to the syntaxin/SNAP-25 labeling combination (Figure 3B), addition of synaptobrevin to the preassembled NN and CC binary complexes entirely eliminated the populations with intermediate FRET. That the intermediate FRET efficiency states could be eliminated with a short 90 min (or even with 30 min; data not shown) incubation demonstrates that our experimental conditions primarily produce the 1:1 binary complex in the supported bilayer, as the dissociation rate of the 2:1 binary complex is substantially longer (Fasshauer et al., 2002).

The effect was less pronounced for the NC label pair, although increased low and high FRET populations (indicating parallel and antiparallel alignment, respectively) are apparent.

This result is consistent with what we observe for the NC reporting labeling combination for the purified ternary SNARE

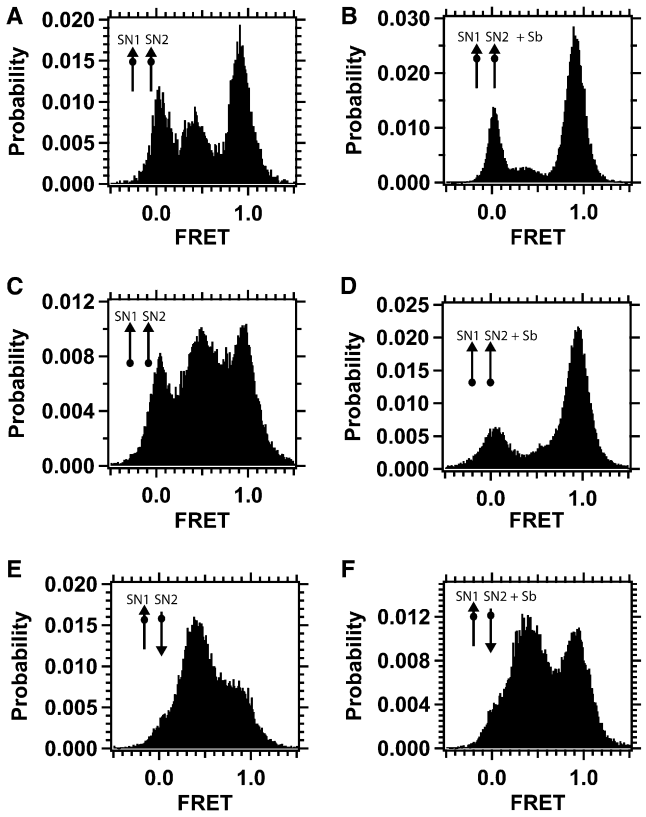

Figure 4. smFRET Population Distributions of Binary Syntaxin/SNAP-25 Complexes with Dyes Attached to SN1 and SN2, and the Effect of the Addition of Synaptobrevin

SNAP-25 (20 nM) labeled with mixtures of Cy3 and Cy5 was incubated over supported lipid bilayers containing unlabeled full-length syntaxin (30 protein molecules/μm^2, similar to the conditions of Figures 1 and 5) for 20 min and then rinsed away. FRET efficiencies for all complexes showing exactly one donor and one acceptor were measured and compiled into histograms. Distributions for all three mutants of SNAP-25, K76C/Q197C (CC in [C]), Q20C/Q197C (NC in [E]), and Q20C/N139C (NN in [A]), show three main populations at low, medium, and high FRET. The high FRET population was the largest for both of the two combinations of labeling sites expected to have high FRET for the parallel configuration, Q20C/N139C (A) and K76C/Q197C (C). For dye positions that are expected to be 8 nm apart if they were an elongated parallel helix bundle, a population with FRET ~0.4 was dominant. In SNAP-25 NN (B), SNAP-25 CC (D), the intermediate FRET population is eliminated by a 90 min incubation of 50 μM synaptobrevin (1–96) over the bilayer containing binary complexes previously formed by binding SNAP-25 to membrane-incorporated, unlabeled syntaxin.

complex (compare Figure S1B and Figure 4F). Thus, there is a population of SNARE complex with antiparallel helices that is stabilized by the interaction with synaptobrevin. Note that there, the majority of complexes are in the parallel configuration (between 60% and 70%; see Figure S1 and accompanying text). We conclude that synaptobrevin is stabilizing both parallel and antiparallel (SN1-SN2) configurations.

Effect of Accessory SNARE-Binding Proteins on the Binary Complex

A number of accessory proteins that interact with syntaxin and SNAP-25 are known to be essential for neurotransmitter release.

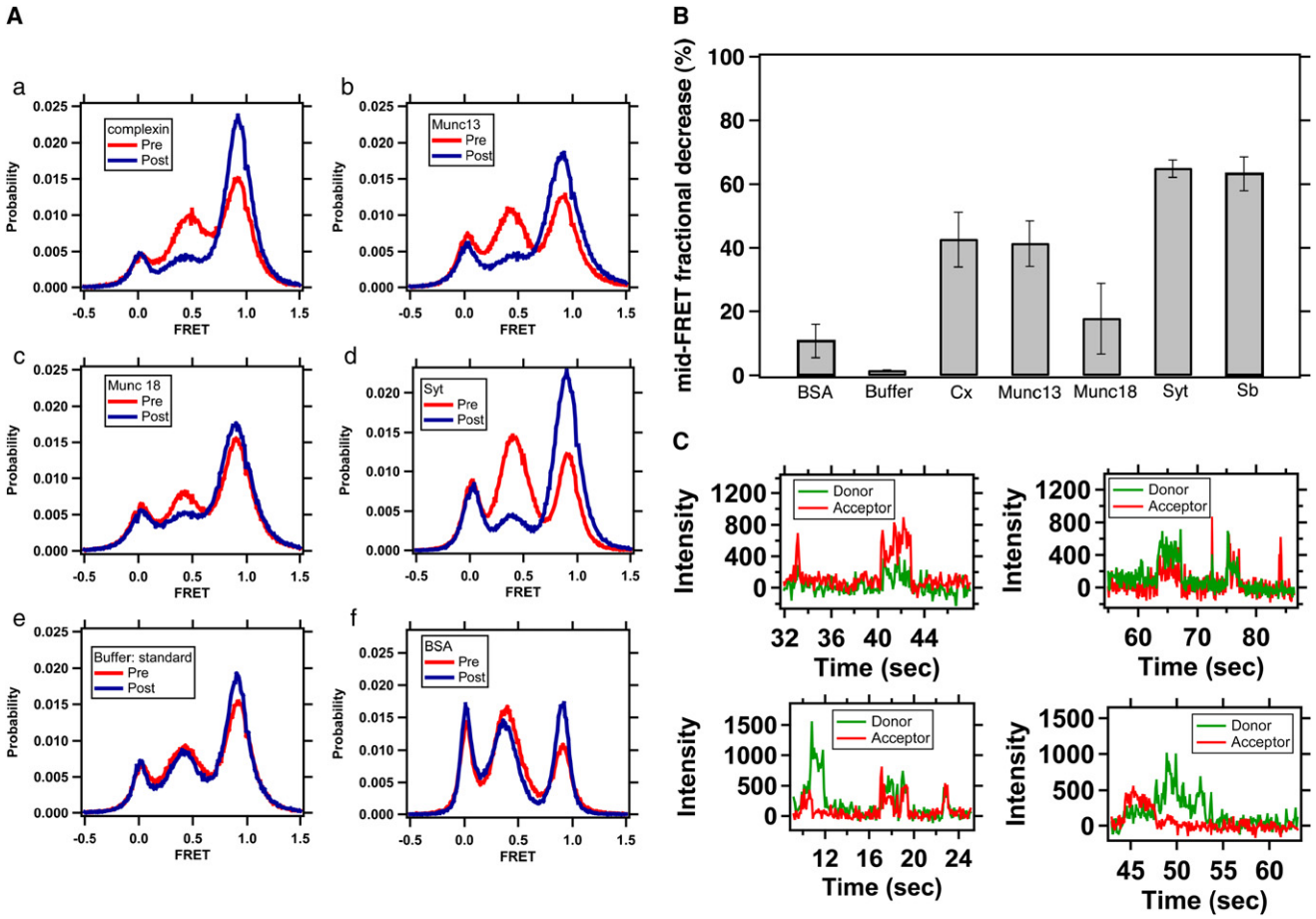

Figure 5. Accessory SNARE-Binding Proteins Alter the Intermediate FRET State of the Binary Complex

(A) FRET distributions are presented for doubly labeled SNAP-25 NN incorporated into binary complexes formed by 30 min incubation of 20 nM SNAP-25 over syntaxin bilayers (30 protein molecules/μm^2). Histograms were acquired immediately before (red) and ~15 min after (blue) addition of 50 μM complexin (a), 5 μM Munc13 (b), 5 μM Munc18 (c), 25 μM synaptotagmin (d), or controls of protein-free imaging buffer (e) or 10 μM BSA (f). Each histogram is the accumulation of three to five independently repeated experiments.

(B) From the histograms in (A), the percent decrease in the fraction of all molecules that were in the mid-FRET states was calculated. The mid-FRET state is defined as events within the FRET efficiency range 0.17–0.65, which are the minima in the valleys between the peaks in all of the accessory protein-free, binary complex experiments (red curves) (i.e., if f = [number of events mid-FRET/total events] for a given histogram, then mid-FRET fractional decrease [%] = $100^*[f_{preaccessory\ protein} - f_{postaccessory\ protein}]/f_{preaccessory\ protein}$). The bars give the average of at least three independently repeated experiments and the full error bar lengths are twice the standard error of the mean. BSA and buffer-only experiments show little effect.

(C) Single-molecule FRET traces between a donor dye (Cy3) at residue 383 of synaptotagmin and an acceptor dye (Cy5) on SNAP-25 NC in bilayer-incorporated binary complexes (in TBS adjusted to contain 50 mM NaCl and 1 mM $CaCl_2$) confirm a direct molecular interaction.

We investigated the effects of complexin, the MUN domain of Munc13, Munc18, and the cytoplasmic domain of synaptotagmin I on the intermediate FRET states that we have reported for the binary complex formed with doubly labeled SNAP-25.

Binary complexes using SNAP-25 NN labeled with both donor and acceptor were formed on syntaxin containing bilayers. A data set was acquired to characterize the binary complex thus formed similar to the conditions and procedures described above (cf Figure 4). Next, a solution containing one of the accessory proteins was introduced into the channel, and a new data set was acquired from the same binary complex containing surface while the accessory protein remained in solution. The normalized FRET distributions measured before and after addition of the accessory proteins are displayed together in Figure 5A for each accessory protein tested in independent experiments. Each histogram is the accumulation of three to five independently repeated experiments. Complexin, Munc13, Munc18, and synaptotagmin I in the absence of Ca^{2+} all decrease the intermediate FRET population in favor of the high FRET, parallel-aligned state. Control experiments, in which protein-free buffer or BSA-containing buffer were used, had little effect on the intermediate FRET state. To quantify the effect of the accessory proteins, we calculated the fractional decrease of the intermediate FRET population upon addition of the indicated proteins (Figure 5B).

The changes in the binary complex FRET states following exposure to the accessory SNARE-binding proteins, but not upon exposure to BSA or protein-free buffer, suggest that each of these accessory proteins has a significant interaction with the binary complex. We sought to verify that interaction by detection of smFRET signals between binary complexes and synaptotagmin

in solution above the bilayer. Binary complexes were prepared in the supported bilayers using SNAP-25 NC that was dye labeled with only the acceptor dye Cy5 rather than the mixture of Cy3 and Cy5 used in the previous sections. We introduced synaptotagmin, labeled at a cysteine mutation in the C2B domain (residue 383) with the donor dye Cy3 (Bowen et al., 2005), into the channel at 1 nM. Such low concentrations are necessary to allow single-molecule level imaging of interactions, so to increase the binding between synaptotagmin and the binary complex, we lowered the salt concentration and augmented the buffer with calcium, conditions first discovered by Tang et al. (2006) for robust synaptotagmin/ternary SNARE complex interactions. With the same alternating laser illumination sequence used above, we identified individual binary complexes on the bilayer by emission of Cy5 under red laser illumination, and then monitored fluorescence from those spots under green illumination. Synaptotagmin was observed to bind at binary complexes with variable levels of FRET (see Figure 5C). The duration of the synaptotagmin-bound state was exponentially distributed with a decay time of 1.6 s. A broad FRET distribution resulted from pooling all binding events (data not shown).

There is some variation of the FRET profiles in the absence of the accessory factors (red curves in Figure 5). This variation is quite typical, as each panel represents a distinct experiment with freshly purified proteins and reconstituted binary complex. Each such process appears to produce somewhat different distributions of the three configurations of the binary complex. However, because the addition of accessory factors is performed on the same respective samples, these experimental variations do not affect our conclusions.

DISCUSSION

SNARE complex formation is an essential step in the fusion of synaptic vesicles and the release of neurotransmitters. In the prevailing model, the binary interaction between syntaxin and SNAP-25 represents the first intermediate in SNARE complex formation. This complex has been called the target (t)-SNARE or acceptor complex because it is predicted to form the binding site for synaptobrevin, which localizes to synaptic vesicles (Jahn and Scheller, 2006; Pobbati et al., 2006). The binding of synaptobrevin to the binary syntaxin/SNAP-25 complex thus serves to closely tether synaptic vesicles near the active zone of the synapse. The assembly of the SNARE complex from three natively unfolded monomers is thought to provide the energy needed to drive membrane fusion. As such, folding of the SNARE complex has been carefully studied. Like other protein folding reactions, the SNARE assembly pathway is filled with local minima and off-pathway states that must be avoided to ensure that membrane fusion occurs. Our previous work showed that SNARE proteins can dock vesicles in a variety of combinations and that SNARE complex assembly could be uncoupled from vesicle docking and fusion (Bowen et al., 2004). However, under those conditions fusion was a rare event, suggesting that the correct folding pathway might be important in coupling SNARE complex formation to vesicle fusion.

Syntaxin and SNAP-25 often form a stable dead-end 2:1 complex in vitro where a second syntaxin SNARE domain takes the usual position of the synaptobrevin helix in the SNARE complex. In PC12 cell assays, formation of 2:1 complexes through the addition of excess syntaxin SNARE domain has a dominant-negative effect on secretion (Chen et al., 2001). The prevalence of this 2:1 species during solution assembly of SNARE proteins made it impossible to study the 1:1 binary complex by bulk methods. In contrast to the neuronal SNAREs, the yeast binary SNARE complex adopts a 1:1 stoichiometry. NMR studies of the yeast SNAREs revealed significant conformational flexibility of the binary t-SNARE complex, although some structure is induced compared to individual SNAREs (Fiebig et al., 1999). It is likely that the neuronal t-SNARE complex exhibits similar flexibility in the 1:1 state. In contrast, the 2:1 state forms a very stable four-helix bundle (Margittai et al., 2001; Xiao et al., 2001; Kim et al., 2002). Using smFRET we have characterized, to our knowledge for the first time, the structure and dynamics of the neuronal binary complex in its 1:1 state, and investigated its interactions with synaptobrevin, complexin, Munc13, Munc18, and synaptotagmin.

Structure and Dynamics of the Neuronal 1:1 Syntaxin/SNAP-25 Complex

The conformation of the 1:1 binary complex is more variable than one would expect if it formed a stable three-helix bundle. With labeling sites in syntaxin and SN1, and dual labeling sites in SNAP-25, we observed dynamic changes in FRET efficiency levels. This included both frame-by-frame variability in FRET efficiency as well as stochastic switching between stable intermediate and high FRET states (Figures 3 and 4). These large changes in FRET efficiency indicate conformational transitions within the binary complex involving large (>5 nm) movements. Some of the intermediate FRET efficiency values can arise from motional averaging over discrete conformational states that occur on a timescale faster than our instrument's integration time (~100 ms).

When the labeling sites were near the same end of the SNAP-25 domains (NN or CC), the distribution is dominated by a high FRET population, indicating that the dyes are in close proximity (Figures 4A and 4C, respectively). This suggests a preference for a parallel configuration for the two SNAP-25 SNARE domains. When the dyes were at opposite ends of the SNAP-25 SNARE domains (NC), most complexes were observed with intermediate to low FRET, suggesting that the N and C termini can sometimes approach within 5 nm of each other, significantly closer than if they were in the extended state of the ternary SNARE complex (~11 nm) (Figure 4E).

Considering the sparse nature of labeling site combinations used for the FRET efficiency measurements, we could only deduce an approximate model of the configurations of the 1:1 binary complex (Figure 6). We propose an equilibrium between three configurations of the binary complex, a configuration consisting of the SNARE domains of syntaxin (SX) and SNAP-25 (SX-SN1-SN2), and two configurations involving the SNARE domain of syntaxin and either one of the two SNAP-25 SNARE domains with the other SNAP-25 domain dissociated (referred to as SX-SN1 and SX-SN2) (Figure 6). The SX-SN1 and SX-SN2 states give rise to the intermediate populations because the dissociated SNAP-25 SNARE domain (SN2 and SN1, respectively) is expected to move on a timescale faster than the time resolution producing average FRET values that vary between FRET = 0 and FRET = 1. The broad distribution of the intermediate state is

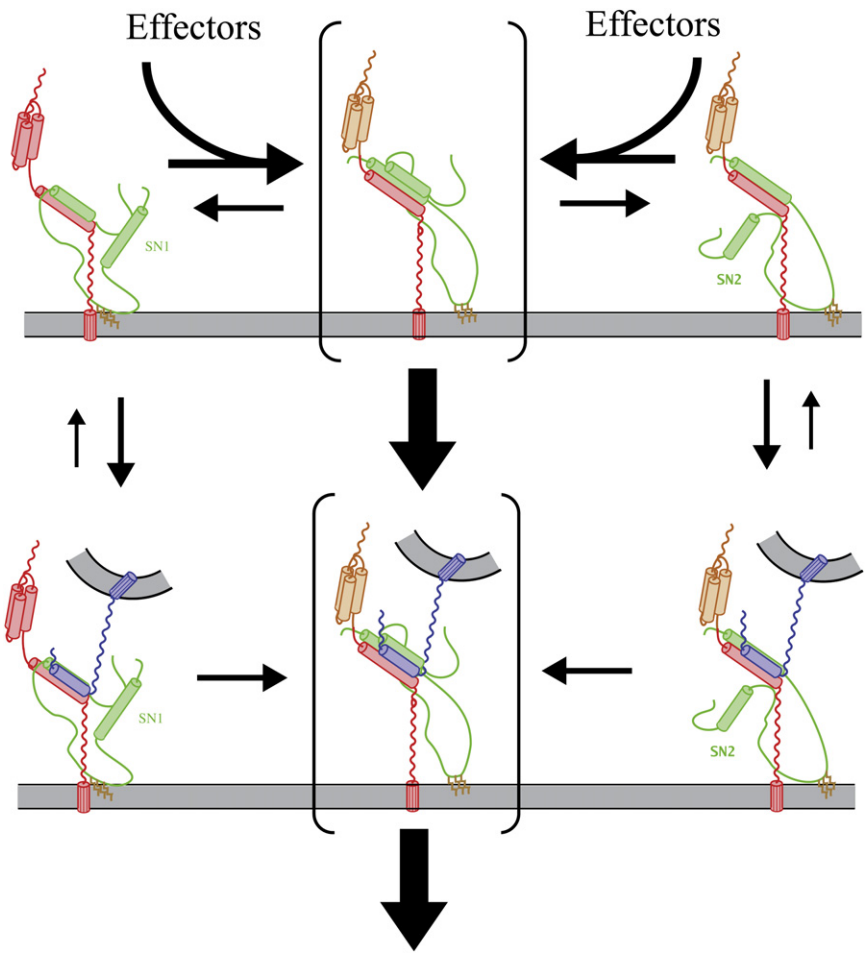

Figure 6. A Model of Conformational Flexibility in the Binary Complex that Would Generate the Intermediate FRET State

The long-lived 1:1 complex between syntaxin and SNAP-25 is drawn as an equilibrium between three distinct configurations (top): (top center in parentheses) both SNAP-25 SNARE domains bound to the syntaxin SNARE domain (SX-SN1-SN2); (top right) only the SN1 domain of SNAP-25 bound to syntaxin (SX-SN1); or (top left) only the SN2 SNAP-25 domain bound to syntaxin (SX-SN2). A stable complex of both SNAP-25 domains tightly bound (SX-SN1-SN2) would lead to stable, high FRET efficiency using our NN and CC FRET labeling combinations. In the cases with one SNAP-25 domain unbound from syntaxin (SX-SN1 or SX-SN2), the free SNAP-25 domain will be in rapid motion relative to the bound domain. With a donor in one domain and an acceptor in the other domain, this rapid motion will lead to widely varying FRET efficiencies that change on timescales faster than the 100 ms integration time of our instrument, resulting in the intermediate FRET values that are measured. Accessory proteins drive the conformational equilibrium from the states with one helix unbound in favor of the state with both helices bound, the synaptobrevin acceptor state.

consistent with sampling of different conformations on a fast timescale. If the intermediate state were in a well-defined unique conformation, it would lead to a much sharper intermediate FRET peak. In vivo palmitoylation of SNAP-25 will likely affect details of the kinetics of switching between the three configurations of the binary complex, although membrane anchoring of the linker region would not outright prevent any of these configurations in the binary complex.

The existence of the SX-SN1 configuration is consistent with observations in PC12 cells using a dual-labeled construct that only contained the SN1 and linker regions of SNAP-25 (An and Almers, 2004). It is also consistent with the ability to form a complex between the syntaxin SNARE domain and SN1 (Misura et al., 2001). However, our data also suggest the presence of an SX-SN2 configuration with the SN1 domain dissociated, as the intermediate FRET state is more pronounced in the experiments with doubly labeled SNAP-25 compared to single-labeled SNAP-25. When comparing Figures 3 and 4, it appears that the intermediate state is much more pronounced for the SN1-SN2 FRET experiments. In fact, the effect is much more than what one would expect if the dynamics between SN2 and syntaxin would be similar to that of SN1 and syntaxin. Thus, we conclude that SN2 has a higher tendency to dissociate from the binary complex.

We believe that the syntaxin N-terminal domain is in the "open" conformation (Dulubova et al., 1999; Munson et al., 2000) in the binary complex because if it were permanently in the closed conformation, it would prevent interactions between syntaxin and SNAP-25, at least in the N-terminal portion of the SNARE domains. Because little difference is observed between N- and C-terminal labeling pairs on SNAP-25 (Figure 4), we can exclude the presence of a permanently closed syntaxin configuration. Could there be a dynamic effect? If syntaxin would dynamically interchange between a closed conformation and an open conformation that can interact with SNAP-25, we would expect Munc18 to siphon away syntaxin from assembled binary complexes because it interacts very tightly with the closed conformation. We do not see such an effect. Rather, upon exposure to Munc18, the surface density of SNAP-25 dye-labeled binary complexes in the supported bilayers remains constant within experimental fluctuations.

We observe transitions between intermediate FRET and FRET = 1 states (Figure 3C and Figure S2), as indicated in our model. It is unlikely that there would be direct transitions between SX-SN1 and SX-SN2. Rather, such transitions would involve the SX-SN1-SN2 configuration as an intermediate state. Having two helices bound as an intermediate step between the single SX-SN1 or SX-SN2 configurations would help keep the SNAP-25 molecule bound to the syntaxin molecule and result in the very low overall observed dissociation rate for the binary complex (off-rate $\sim$0.005 $\pm$ 0.004 hr^{-1}).

SNAP-25 Domain Swap Does Not Occur

SNAREs were proposed to form oligomers joined by the linker between domain-swapped SNAP-25 SNARE motifs (Fasshauer et al., 1998b; Kweon et al., 2002) possibly involving complexin

(Tokumaru et al., 2001), although this particular observation has been disputed (Pabst et al., 2002). Furthermore, the linker is functionally dispensable in a PC12 cell-based assay for neurotransmitter release (Chen et al., 1999). To determine the likelihood for a SNAP-25 domain swap in SNARE complexes, we carried out experiments with a mixture of acceptor- and donor-labeled SNAP-25 molecules added to syntaxin, and analyzed the resulting binary complexes. We did not observe any significant population of complexes that exhibited high FRET (~0.4%); in other words, the probability of SNAP-25 domain swapping is extremely low. Thus, it is unlikely that SNAP-25 domain swapping plays a role in a putative higher-order oligomer of the SNARE complex.

Effect on Intermediate State upon Addition of Synaptobrevin

Upon addition of synaptobrevin, the equilibrium shifts predominantly toward the SX-SN1-SN2 configuration (Figure 6). This effect occurs on a fast scale (90 min in Figure 4, and 30 min in data not shown), significantly faster than the published rate constants for synaptobrevin binding to the 2:1 binary complex (Pobbati et al., 2006). Addition of synaptobrevin to the 1:1 binary complex also completely eliminated dynamic variability in FRET efficiency levels and stochastic switching. These changes were observed with all labeling site combinations. The resulting distributions after synaptobrevin addition are similar to the ternary SNARE complex formed using these same labeling sites (Figure S1; Weninger et al., 2003). Thus, the binary complex that we observe is biologically active and forms proper SNARE complexes.

Effect on Intermediate State upon Addition of Other Factors

Surprisingly, we also observed a significant reduction of the intermediate state of the binary complex upon addition the accessory proteins complexin, Munc13, Munc18, and synaptotagmin, but not buffer or BSA controls (Figure 5). All experiments used protein concentrations above the published dissociation constant for each accessory protein, so the relative magnitude of the change in FRET distribution reflects a differential effect of that protein on the dynamics of the binary complex.

There is clear evidence that complexin interacts with the ternary SNARE complex (Chen et al., 2002; Pabst et al., 2002). However, no interaction was detected between complexin and the individual SNAREs or the binary complex by using isothermal titration calorimetry in solution (Pabst et al., 2002). In these experiments, the binary complex was likely in the 2:1 state as characterized by multiangle laser light scattering (Fasshauer et al., 1997b), which might have prevented complexin binding. Furthermore, the N-terminal accessory helix of complexin (residues 29–48) has an inhibitory effect on neurotransmitter release, suggesting that this region can be a placeholder for the C-terminal portion of the synaptobrevin SNARE motif, thereby regulating assembly of the SNARE complex (Xue et al., 2007). This model thus implies an interaction between complexin and the binary complex. Our results now confirm a direct interaction between complexin and the 1:1 binary complex, and that this interaction dramatically stabilizes the SX-SN1-SN2 configuration.

The MUN domain of Munc13 that we studied here is α helical as determined by circular dichroism and has been shown to be sufficient for rescuing neurotransmitter release in hippocampal neurons lacking Munc13s (Basu et al., 2005). It does not interact with syntaxin alone, but we find an interaction with the binary complex that has a similarly pronounced effect as complexin leading to stabilization of the SX-SN1-SN2 configuration. Interestingly, both the SNARE-interacting domain of complexin and the MUN domain of Munc13 are highly α helical, so their strong effect on diminishing the SX-SN1 and SX-SN2 configurations could be explained by stabilization of the SX-SN1-SN2 complex by four-helix bundle formation.

The cytosolic domain of synaptotagmin I contains two conserved Ca^{2+}-binding domains (Perin et al., 1991), C2A and C2B, that interact, in a Ca^{2+}-dependent manner with acidic lipids, and both in a Ca^{2+}-dependent and -independent manner with SNAP-25 and syntaxin, the binary complex, and the ternary SNARE complex (Bai and Chapman, 2004; Südhof, 2004; Rizo et al., 2006). The possibility of simultaneous binding to both membrane and SNARE complex was first proposed based on low-resolution smFRET measurements between synaptotagmin and the ternary SNARE complex (Bowen et al., 2005), and has recently been actually observed (Dai et al., 2007). The precise physiological meaning of these interactions and their role in Ca^{2+}-triggered neurotransmitter release are still unclear. We now observe a direct interaction between synaptotagmin I and the binary complex. Our results using the doubly labeled SNAP-25 FRET reporter incorporated into the binary complex indicate that synaptotagmin I stabilizes the three-helix bundle configuration SX-SN1-SN2 to the same extent as synaptobrevin, even in the absence of Ca^{2+}. We further used FRET between acceptor-labeled binary complex and donor-labeled synaptotagmin to directly confirm the molecular interaction. Consistent with the observed stabilization of the three-helix bundle configuration, recent cross-linking studies between the C2AB fragment of synaptotagmin I and SNAP-25 have revealed interactions with both SN1 and SN2 (Lynch et al., 2007). Our observed stabilization of the binary t-SNARE complex explains the large increase in the extent of lipid mixing in bulk assays with reconstituted SNAREs in liposomes upon addition of C2AB and then, after an incubation period, Ca^{2+} (Stein et al., 2007; Tucker et al., 2004) (Ed Chapman, personal communication). However, because synaptotagmin I and the binary complex are thought to reside primarily on opposite membranes, this interaction could take place only if the synaptic vesicle is sufficiently close to the target membrane.

Sec1/Munc18 (SM) proteins are a small family of cytoplasmic proteins that play an important but poorly understood role in intracellular membrane fusion. Interactions between the neuronal SM protein Munc18 and syntaxin (Hata et al., 1993; Misura et al., 2000), the binary t-SNARE complex (Zilly et al., 2006), and the ternary SNARE complex have been found (Dulubova et al., 2007). Based on the available structural and biophysical information, several possible interaction interfaces and conformations have been found: a tight interaction between the closed form of syntaxin and Munc18 involving part of the syntaxin SNARE motif, and the N-terminal domain of syntaxin (Misura et al., 2000), as well as interactions between the SNARE domains of the ternary complex and the short N-terminal sequence of syntaxin (Bracher et al., 2002; Dulubova et al., 2007). We now observe interactions between the MUN domain of Munc18 and the 1:1 binary complex accompanied by stabilization of the SX-SN1-SN2 configuration. However, in contrast to the other accessory proteins tested, the

effect on the configurations of the binary complex is highly variable. This variability might be related to the several distinct binding modes between Munc18 and syntaxin. Although we do not see any evidence for Munc18 displacing SNAP-25 and inducing the closed conformation of syntaxin, it is conceivable that some Munc18 interactions only involve the N-terminal sequence of syntaxin without affecting the SNARE domains and thus no effect on the intermediate FRET states, whereas other binding modes would directly affect the SNARE domains, leading to the stabilization of the SX-SN1-SN2 configuration.

Concluding Remarks

We conclude that in the cellular environment the binary complex will be primarily in the SX-SN1-SN2 configuration because there is a high likelihood that at least one of the accessory proteins is near a particular t-SNARE complex. Because it is the SX-SN1-SN2 configuration to which synaptobrevin can readily bind, the formation of this configuration of the t-SNARE complex is likely not going to a limiting step in neurotransmitter release. Progression from this acceptor complex to the four-helix bundle might be the only folding pathway that leads to membrane fusion (Figure 6, top and bottom center in parentheses). Synaptobrevin might interact with the helix unbound states of the binary complex, but these complexes would be delayed in folding until reassociation of the missing SNAP-25 helix (bottom left and right). Thus, although these complexes could transition to four-helix bundles and dock vesicles, this alternate folding pathway would inefficiently couple the folding reaction to membrane fusion.

The dynamic nature of the t-SNARE complex might also account for some of the variability observed in many in vitro experiments. It has been suggested that "SNARE proteins are powerful but hapless, unable to channel the energy released by their complex formation, and need to be organized by Rab and SM proteins" (Südhof, 2007). This study shows that several of the factors identified as important for Ca^{2+}-triggered vesicle release have an effect on the structure and dynamics of a key intermediate in the SNARE assembly pathway. It might be that by making the 1:1 binary complex a better acceptor for synaptobrevin, the energy associated with the correct folding pathway becomes available to catalyze the merger of the two bilayers.

EXPERIMENTAL PROCEDURES

Proteins and Lipid Bilayers

Plasmids, protein expression, and protein purification for full-length syntaxin, full-length SNAP-25, full-length synaptobrevin, synaptobrevin fragment (1–96), complexin, and synaptotagmin I C2AB (residues 96–421, T383C) have been described previously (Weninger et al., 2003; Bowen et al., 2004, 2005). Briefly, all proteins were expressed as hexa-His fusions in pet28 (Novagen) (except synaptotagmin, which was a GST fusion in pGex4T1) and were purified by a combination of metal-affinity (except synaptotagmin, glutathione resin affinity), ion-exchange, and gel-filtration chromatography. Transmembrane proteins were extracted in Thesit and transferred to β-octyl glucoside before reconstitution.

The expression construct for hexa-His-tagged Munc18 was a kind gift from Doug Hattendorf and William Weis (Misura et al., 2000). Protein was expressed in BL21(DE3) cells and purified by Ni-NTA affinity according to the manufacturer's instructions (QIAGEN). The eluted protein was dialyzed into 20 mM Tris (pH 7.8), 200 mM NaCl, 1 mM DTT, and was 90% pure as assessed by SDS-PAGE. Samples (5–10 μM) of Munc18 were stored at 4°C and used for single-molecule experiments within 4 days of Ni-NTA purification.

Purified protein samples of the MUN domain of Munc13 (Basu et al., 2005) were a generous gift of Jose Rizo and Yibin Xu. The protein sample was purified by ion-exchange and gel-filtration chromatography. SDS-PAGE was used to check the homogeneity of the sample. The protein concentration was initially 20 μM, and was diluted to 5 μM for binding experiments.

Three different combinations of double cysteine mutations (Q20C/N139C, Q20C/Q197C, and K76C/Q197C) were introduced into a cysteine-free SNAP-25 template by the QuikChange method (Stratagene). The ternary SNARE complex (Figure S1) was purified with or without a urea step as described previously (Weninger et al., 2003). Briefly, the hexa-His tag was left on synaptobrevin, which allows for metal-affinity chromatography to isolate the SNARE complex followed by anion exchange in order to remove free synaptobrevin.

Our general protocol for dye labeling of syntaxin and synaptobrevin at suitable sites has been described elsewhere (Weninger et al., 2003; Bowen et al., 2004, 2005). Briefly, it involves incubation of proteins with maleimide dyes (Cy dyes, GE Healthcare, unless noted otherwise) at pH 7.4 followed by gel filtration and dialysis to remove free dye. We used the following modification for the double dye species labeling of SNAP-25. The two cysteine residues in the SNAP-25 double mutants were labeled with a mixture of maleimide-derivatized donor (Cy3) and acceptor (Cy5) dyes by simultaneously mixing the protein with both dyes, each at a 10-fold molar excess over protein. Donor and acceptor dyes randomly bound to all cysteines yielding three populations of doubly labeled proteins, one with two donors, a second with two acceptors, and a third with one donor and one acceptor. Our analysis protocol of the smFRET data was designed to select only those molecules with exactly one donor and one acceptor. Labeling efficiencies for SNAP-25 were typically greater than 80% as assessed by UV-vis absorption spectroscopy.

Experiments were performed with custom-built quartz flow cells. Supported lipid bilayers were formed by spontaneous condensation of liposomes. Reconstitution of membrane proteins into preformed liposomes was accomplished by detergent depletion followed by size exclusion on Sepharose CL-4B to remove free protein (Weninger et al., 2003).

Because unlabeled protein is not directly observable, the concentration of unlabeled syntaxin incorporated into the supported lipid bilayers was estimated from the protein-to-lipid ratio used during reconstitution. The reconstitution efficiency is less than 100%, and approximately 50% of reconstituted protein ends up oriented toward the optical surface in the final supported bilayers as assessed by susceptibility to proteases (Bowen et al., 2004). Thus, the concentration of correctly inserted syntaxin in the bilayer is significantly overestimated. All lipid bilayers and liposomes in this work were formed from egg phosphatidylcholine (EggPC) purchased from Avanti Polar Lipids.

Fluorescence Measurements

smFRET efficiency measurements were made with a prism-type, total internal reflection microscope equipped with either a Pentamax CCD (Roper Scientific) or Cascade EMCCD (Princeton Instruments) as described previously (Weninger et al., 2003; Bowen et al., 2004, 2005; Li et al., 2007). Single-molecule observations in Figure 1 were made under steady red laser (635 nm) illumination. In Figures 2 and 3, steady green laser (532 nm) was used. For Figures 4 and 5 and Figure S1, an alternating laser illumination sequence (0–1 s at 635 nm; 1.5–46 s at 532 nm; 47–57 s at 635 nm) allowed us to diagnose the number of acceptor and donor dyes at each molecule independent of any possible FRET. Between 1 and 1.5 s, laser shutters were active so this period was excluded from the analysis.

All FRET efficiency measurements (except studies in Figure 5C) were carried out at room temperature in 20 mM Tris (pH 7.8), 200 mM NaCl, 1 mM DTT, 2% glucose (w/v), 100 μM cyclooctatetraene, supplemented with an enzymatic oxygen scavenger mixture consisting of glucose oxidase (Sigma) 100 units/ml and catalase (Sigma) 1000 units/ml. Studies of FRET between acceptor-labeled binary complex and donor-labeled synaptotagmin (Figure 5C) used the same oxygen-scavenging buffer with the following modifications: NaCl was 50 mM and $CaCl_2$ was present at 1 mM. Experiments with accessory proteins in solution were prepared by mixing equal volumes of doubly concentrated observation buffer into protein solutions to achieve constant oxygen-scavenging mixtures for all observations.

Measured emission intensity values were corrected for background fluorescence ($I' = I_{measured} - I_{background}$) and leakage of 7% of the donor intensity into the acceptor channel. FRET efficiency was calculated from the

background-corrected measurements of acceptor emission ($I'_{acceptor}$) and donor emission (I'_{donor}) as FRET = $I'_{acceptor}/(I'_{acceptor} + I'_{donor})$.

Histograms were compiled from the measured FRET efficiency observed in individual time traces. In Figure 3, histograms show frame-by-frame FRET efficiency for complexes that showed nonzero FRET within the first second of the observation period. These histograms were compiled over the entire duration of the time traces. Thus, these histograms represent the probability that a binary complex will display a given FRET efficiency state during the course of the experiment. Histograms in Figures 4 and 5 contain frame-by-frame FRET values for the time when exactly one donor and one acceptor were confirmed to be present at a complex and not bleached. The histogram in Figure S1 shows a five-frame average FRET efficiency value calculated over the first half-second of green laser illumination for all single donor/acceptor dye pairs, and thus represents the number of complexes that were observed at a given FRET efficiency state from an ensemble of particles.

Syntaxin Monodispersity in Supported Bilayers

Syntaxin was reconstituted into vesicles at submicromolar concentrations, which is below the reported micromolar K_D for self-interaction (Lerman et al., 2000). In order to achieve lateral separation between dye-labeled molecules in the bilayer greater than the optical resolution of the microscope, vesicles containing syntaxin were diluted with protein-free vesicles before bilayer deposition. We obtained roughly 73 ± 30 syntaxin molecules in the 4050 μm^2 observation field when using a protein-to-lipid ratio of $1{:}10^6$ or $1{:}10^7$ during reconstitution. To confirm that syntaxin is largely monomeric under these conditions, we observed the fluorescence intensity of labeled syntaxin at each spot in the microscope image under extended red laser illumination. The number of dyes present in an observed spot was derived from the number of discrete steps observed in the decay of fluorescence emission to baseline (Figure 1, inset).

To limit the possibility that experimental factors affected monodispersity, we tested labeling sites in the N and C termini of syntaxin, labeling with Alexa dyes (Invitrogen) or Cy dyes (GE Healthcare) and the effect of Ca^{2+} and/or EDTA. None of these factors affected the distribution of the frequency of occurrence for a specified number of dyes in observed spots, so we used an average of all distributions in the subsequent analysis (Figure 1). The frequency of occurrence of one or two dyes had to be corrected for partial labeling of syntaxin in order to obtain the true probability β that two syntaxin molecules (labeled or unlabeled) colocalize in a particular spot. The fraction of labeled syntaxin molecules (α) ranged from 40% to 65% as determined from the ratio of dye peak absorbance to 280 nm absorbance (corrected for dye absorbance) measured with UV-vis spectroscopy. The vast majority (~99%) of the spots contain single or double dyes (Figure 1). Thus, we neglected triplet and higher-order species in the following analysis.

The observed probability R of experimentally detecting two dyes at a given spot was determined from the results shown in Figure 1 by

$$R = \frac{D_{obs}}{S_{obs} + D_{obs}},$$

where S_{obs} is the number of observed spots with single dyes and D_{obs} is the number of observed spots with two dyes. From this, we obtain R = 0.154 ± 0.032.

The occurrence of one dye in an observed spot can result from labeled singles or from doubles with one labeled molecule and one unlabeled molecule. Thus, the probability of occurrence of a single dye in a spot is

$$S = (1 - \beta)\alpha + 0.5\beta\alpha(1 - \alpha).$$

The probability of occurrence of two dyes in an observed spot is

$$D = 0.5\beta\alpha^2.$$

We can express R in terms of the labeling efficiency (α) and colocalization probability (β) as

$$R = \frac{D}{S + D}.$$

This equation can be solved for the colocalization probability β as a function of R to yield

$$\beta = \frac{R}{0.5(\alpha + R)}.$$

Using the measured labeling efficiency and the experimental R value, we obtain a colocalization probability β = 0.51 ± 0.14. Thus, about 50% of the syntaxin molecules are isolated singles. The remaining spots may contain colocalized syntaxin. However, colocalization does not imply that two syntaxin molecules actually interact.

To determine whether there is any interaction between two syntaxin molecules, we calculated a theoretical prediction that is derived from considering the frequency that two molecules will randomly land at the same location. For N molecules randomly distributed on an area of the bilayer A_{screen}, the population average that two molecules are located within the observed spot with area A_{spot} around a single molecule is calculated as

$$P(2dyes) = N\left(\frac{A_{spot}}{A_{screen}}\right),$$

the population average of three dyes in an observed spot is

$$P(3dyes) = N(N-1)\left(\frac{A_{spot}}{A_{screen}}\right)^2,$$

and so on. A somewhat higher fraction of doubles is observed in the experiment than is expected from random colocalization (Figure 1), so there might be a small fraction of interacting syntaxin molecules. As shown above, the fraction of colocalized syntaxin (labeled or unlabeled) molecules does not exceed 50%. Because the mobility of syntaxin molecules is restricted in our supported bilayers (Bowen et al., 2004), we conclude that at least 50% of syntaxin molecules will form 1:1 complexes upon addition of SNAP-25.

Supplemental Data

Supplemental Data include two figures and can be found with this article online at http://www.structure.org/cgi/content/full/16/2/308/DC1/.

ACKNOWLEDGMENTS

We thank Doug Hattendorf, William Weis, and Jose Rizo for stimulating discussions, Yibin Xu for providing a purified sample of the MUN domain of Munc13, and Jennifer Alyono, Anton Rosenbaum, Winston Odin, and Barry Wilk for technical assistance. This work was supported in part by National Institutes of Health grant MH63105 to A.T.B., and by grants of the National Science Foundation, Air Force Office of Scientific Research, and NASA to S.C. The research of K.W. is supported in part by a Career Award at the Scientific Interface from the Burroughs Wellcome Fund.

Received: December 13, 2007
Revised: December 13, 2007
Accepted: December 17, 2007
Published: February 12, 2008

REFERENCES

An, S.J., and Almers, W. (2004). Tracking SNARE complex formation in live endocrine cells. Science *306*, 1042–1046.

Bai, J., and Chapman, E.R. (2004). The C2 domains of synaptotagmin—partners in exocytosis. Trends Biochem. Sci. *29*, 143–151.

Basu, J., Shen, N., Dulubova, I., Lu, J., Guan, R., Guryev, O., Grishin, N.V., Rosenmund, C., and Rizo, J. (2005). A minimal domain responsible for Munc13 activity. Nat. Struct. Mol. Biol. *12*, 1017–1018.

Bowen, M.E., Engelman, D.M., and Brunger, A.T. (2002). Mutational analysis of synaptobrevin transmembrane domain oligomerization. Biochemistry *41*, 15861–15866.

Bowen, M.E., Weninger, K., Brunger, A.T., and Chu, S. (2004). Single molecule observation of liposome-bilayer fusion thermally induced by soluble N-ethyl maleimide sensitive-factor attachment protein receptors (SNAREs). Biophys. J. *87*, 3569–3584.

Bowen, M.E., Weninger, K., Ernst, J., Chu, S., and Brunger, A.T. (2005). Single-molecule studies of synaptotagmin and complexin binding to the SNARE complex. Biophys. J. *89*, 690–702.

Bracher, A., Kadlec, J., Betz, H., and Weissenhorn, W. (2002). X-ray structure of a neuronal complexin-SNARE complex from squid. J. Biol. Chem. *277*, 26517–26523.

Brunger, A.T. (2005). Structure and function of SNARE and SNARE-interacting proteins. Q. Rev. Biophys. *38*, 1–47.

Chapman, E.R., An, S., Barton, N., and Jahn, R. (1994). SNAP-25, a t-SNARE which binds to both syntaxin and synaptobrevin via domains that may form coiled coils. J. Biol. Chem. *269*, 27427–27432.

Chen, Y.A., Scales, S.J., Patel, S.M., Doung, Y.C., and Scheller, R.H. (1999). SNARE complex formation is triggered by Ca^{2+} and drives membrane fusion. Cell *97*, 165–174.

Chen, Y.A., Scales, S.J., and Scheller, R.H. (2001). Sequential SNARE assembly underlies priming and triggering of exocytosis. Neuron *30*, 161–170.

Chen, X., Tomchick, D.R., Kovrigin, E., Arac, D., Machius, M., Südhof, T.C., and Rizo, J. (2002). Three-dimensional structure of the complexin/SNARE complex. Neuron *33*, 397–409.

Dai, H., Shen, N., Arac, D., and Rizo, J. (2007). A quaternary SNARE-synaptotagmin-Ca^{2+}-phospholipid complex in neurotransmitter release. J. Mol. Biol. *367*, 848–863.

Dennison, S.M., Bowen, M.E., Brunger, A.T., and Lentz, B.R. (2006). Neuronal SNAREs do not trigger fusion between synthetic membranes but do promote PEG-mediated membrane fusion. Biophys. J. *90*, 1661–1675.

Dulubova, I., Sugita, S., Hill, S., Hosaka, M., Fernandez, I., Südhof, T.C., and Rizo, J. (1999). A conformational switch in syntaxin during exocytosis: role of munc18. EMBO J. *18*, 4372–4382.

Dulubova, I., Khvotchev, M., Liu, S., Huryeva, I., Südhof, T.C., and Rizo, J. (2007). Munc18-1 binds directly to the neuronal SNARE complex. Proc. Natl. Acad. Sci. USA *104*, 2697–2702.

Duman, J.G., and Forte, J.G. (2003). What is the role of SNARE proteins in membrane fusion? Am. J. Physiol. Cell Physiol. *285*, C237–C249.

Ernst, J.A., and Brunger, A.T. (2003). High resolution structure, stability, and synaptotagmin binding of a truncated neuronal SNARE complex. J. Biol. Chem. *278*, 8630–8636.

Fasshauer, D., and Margittai, M. (2004). A transient N-terminal interaction of SNAP-25 and syntaxin nucleates SNARE assembly. J. Biol. Chem. *279*, 7613–7621.

Fasshauer, D., Bruns, D., Shen, B., Jahn, R., and Brunger, A.T. (1997a). A structural change occurs upon binding of syntaxin to SNAP-25. J. Biol. Chem. *272*, 4582–4590.

Fasshauer, D., Otto, H., Eliason, W.K., Jahn, R., and Brunger, A.T. (1997b). Structural changes are associated with soluble N-ethylmaleimide-sensitive fusion protein attachment protein receptor complex formation. J. Biol. Chem. *272*, 28036–28041.

Fasshauer, D., Eliason, W.K., Brunger, A.T., and Jahn, R. (1998a). Identification of a minimal core of the synaptic SNARE complex sufficient for reversible assembly and disassembly. Biochemistry *37*, 10354–10362.

Fasshauer, D., Sutton, R.B., Brunger, A.T., and Jahn, R. (1998b). Conserved structural features of the synaptic fusion complex: SNARE proteins reclassified as Q- and R-SNAREs. Proc. Natl. Acad. Sci. USA *95*, 15781–15786.

Fasshauer, D., Antonin, W., Margittai, M., Pabst, S., and Jahn, R. (1999). Mixed and non-cognate SNARE complexes. Characterization of assembly and biophysical properties. J. Biol. Chem. *274*, 15440–15446.

Fasshauer, D., Antonin, W., Subramaniam, V., and Jahn, R. (2002). SNARE assembly and disassembly exhibit a pronounced hysteresis. Nat. Struct. Biol. *9*, 144–151.

Fiebig, K.M., Rice, L.M., Pollock, E., and Brunger, A.T. (1999). Folding intermediates of SNARE complex assembly. Nat. Struct. Biol. *6*, 117–123.

Fix, M., Melia, T.J., Jaiswal, J.K., Rappoport, J.Z., You, D., Söllner, T.H., and Rothman, J.E. (2004). Imaging single membrane fusion events mediated by SNARE proteins. Proc. Natl. Acad. Sci. USA *101*, 7311–7316.

Foster, L.J., Yeung, B., Mohtashami, M., Ross, K., Trimble, W.S., and Klip, A. (1998). Binary interactions of the SNARE proteins syntaxin-4, SNAP23, and VAMP-2 and their regulation by phosphorylation. Biochemistry *37*, 11089–11096.

Hata, Y., Slaughter, C.A., and Südhof, T.C. (1993). Synaptic vesicle fusion complex contains unc-18 homologue bound to syntaxin. Nature *366*, 347–351.

Humeau, Y., Doussau, F., Grant, N.J., and Poulain, B. (2000). How botulinum and tetanus neurotoxins block neurotransmitter release. Biochimie *82*, 427–446.

Jackson, M.B., and Chapman, E.R. (2006). Fusion pores and fusion machines in Ca^{2+}-triggered exocytosis. Annu. Rev. Biophys. Biomol. Struct. *35*, 135–160.

Jahn, R., and Scheller, R.H. (2006). SNAREs—engines for membrane fusion. Nat. Rev. Mol. Cell Biol. *7*, 631–643.

Kidokoro, Y. (2003). Roles of SNARE proteins and synaptotagmin I in synaptic transmission: studies at the *Drosophila* neuromuscular synapse. Neurosignals *12*, 13–30.

Kim, C.S., Kweon, D.H., and Shin, Y.K. (2002). Membrane topologies of neuronal SNARE folding intermediates. Biochemistry *41*, 10928–10933.

Kroch, A.E., and Fleming, K.G. (2006). Alternate interfaces may mediate homomeric and heteromeric assembly in the transmembrane domains of SNARE proteins. J. Mol. Biol. *357*, 184–194.

Kweon, D.H., Chen, Y., Zhang, F., Poirier, M., Kim, C.S., and Shin, Y.K. (2002). Probing domain swapping for the neuronal SNARE complex with electron paramagnetic resonance. Biochemistry *41*, 5449–5452.

Laage, R., Rohde, J., Brosig, B., and Langosch, D. (2000). A conserved membrane-spanning amino acid motif drives homomeric and supports heteromeric assembly of presynaptic SNARE proteins. J. Biol. Chem. *275*, 17481–17487.

Lang, T., Margittai, M., Holzler, H., and Jahn, R. (2002). SNAREs in native plasma membranes are active and readily form core complexes with endogenous and exogenous SNAREs. J. Cell Biol. *158*, 751–760.

Lerman, J.C., Robblee, J., Fairman, R., and Hughson, F.M. (2000). Structural analysis of the neuronal SNARE protein syntaxin-1A. Biochemistry *39*, 8470–8479.

Li, Y., Augustine, G.J., and Weninger, K. (2007). Kinetics of complexin binding to the SNARE complex: correcting single molecule FRET measurements for hidden events. Biophys. J. *93*, 2178–2187.

Liu, T., Tucker, W.C., Bhalla, A., Chapman, E.R., and Weisshaar, J.C. (2005). SNARE-driven, 25-millisecond vesicle fusion in vitro. Biophys. J. *89*, 2458–2472.

Liu, W., Montana, V., Bai, J., Chapman, E.R., Mohideen, U., and Parpura, V. (2006). Single molecule mechanical probing of the SNARE protein interactions. Biophys. J. *91*, 744–758.

Lynch, K.L., Gerona, R.R., Larsen, E.C., Marcia, R.F., Mitchell, J.C., and Martin, T.F. (2007). Synaptotagmin C2A loop 2 mediates Ca^{2+}-dependent SNARE interactions essential for Ca^{2+}-triggered vesicle exocytosis. Mol. Biol. Cell *18*, 4957–4968.

Margittai, M., Fasshauer, D., Pabst, S., Jahn, R., and Langen, R. (2001). Homo- and heterooligomeric SNARE complexes studied by site-directed spin labeling. J. Biol. Chem. *276*, 13169–13177.

Misura, K.M., Scheller, R.H., and Weis, W.I. (2000). Three-dimensional structure of the neuronal-Sec1-syntaxin 1a complex. Nature *404*, 355–362.

Misura, K.M., Gonzalez, L.C., Jr., May, A.P., Scheller, R.H., and Weis, W.I. (2001). Crystal structure and biophysical properties of a complex between the N-terminal SNARE region of SNAP25 and syntaxin 1a. J. Biol. Chem. *276*, 41301–41309.

Munson, M., Chen, X., Cocina, A.E., Schultz, S.M., and Hughson, F.M. (2000). Interactions within the yeast t-SNARE Sso1p that control SNARE complex assembly. Nat. Struct. Biol. *7*, 894–902.

Nicholson, K.L., Munson, M., Miller, R.B., Filip, T.J., Fairman, R., and Hughson, F.M. (1998). Regulation of SNARE complex assembly by an N-terminal domain of the t-SNARE Sso1p. Nat. Struct. Biol. *5*, 793–802.

Pabst, S., Margittai, M., Vainius, D., Langen, R., Jahn, R., and Fasshauer, D. (2002). Rapid and selective binding to the synaptic SNARE complex suggests

a modulatory role of complexins in neuroexocytosis. J. Biol. Chem. *277*, 7838–7848.

Perin, M.S., Brose, N., Jahn, R., and Südhof, T.C. (1991). Domain structure of synaptotagmin (p65). J. Biol. Chem. *266*, 623–629.

Pevsner, J., Hsu, S.C., Braun, J.E., Calakos, N., Ting, A.E., Bennett, M.K., and Scheller, R.H. (1994). Specificity and regulation of a synaptic vesicle docking complex. Neuron *13*, 353–361.

Pobbati, A.V., Stein, A., and Fasshauer, D. (2006). N- to C-terminal SNARE complex assembly promotes rapid membrane fusion. Science *313*, 673–676.

Rizo, J., Chen, X., and Arac, D. (2006). Unraveling the mechanisms of synaptotagmin and SNARE function in neurotransmitter release. Trends Cell Biol. *16*, 339–350.

Schoch, S., Deak, F., Konigstorfer, A., Mozhayeva, M., Sara, Y., Südhof, T.C., and Kavalali, E.T. (2001). SNARE function analyzed in synaptobrevin/VAMP knockout mice. Science *294*, 1117–1122.

Söllner, T., Bennett, M.K., Whiteheart, S.W., Scheller, R.H., and Rothman, J.E. (1993). A protein assembly-disassembly pathway in vitro that may correspond to sequential steps of synaptic vesicle docking, activation, and fusion. Cell *75*, 409–418.

Stein, A., Radhakrishnan, A., Riedel, D., Fasshauer, D., and Jahn, R. (2007). Synaptotagmin activates membrane fusion through a Ca(2+)-dependent *trans* interaction with phospholipids. Nat. Struct. Mol. Biol. *14*, 904–911.

Stevens, C.F. (2003). Neurotransmitter release at central synapses. Neuron *40*, 381–388.

Südhof, T.C. (2004). The synaptic vesicle cycle. Annu. Rev. Neurosci. *27*, 509–547.

Südhof, T.C. (2007). Membrane fusion as a team effort. Proc. Natl. Acad. Sci. USA *104*, 13541–13542.

Sutton, R.B., Fasshauer, D., Jahn, R., and Brunger, A.T. (1998). Crystal structure of a SNARE complex involved in synaptic exocytosis at 2.4 Å resolution. Nature *395*, 347–353.

Tang, J., Maximov, A., Shin, O.H., Dai, H., Rizo, J., and Südhof, T.C. (2006). A complexin/synaptotagmin 1 switch controls fast synaptic vesicle exocytosis. Cell *126*, 1175–1187.

Tokumaru, H., Umayahara, K., Pellegrini, L.L., Ishizuka, T., Saisu, H., Betz, H., Augustine, G.J., and Abe, T. (2001). SNARE complex oligomerization by synaphin/complexin is essential for synaptic vesicle exocytosis. Cell *104*, 421–432.

Tucker, W.C., Weber, T., and Chapman, E.R. (2004). Reconstitution of Ca^{2+}-regulated membrane fusion by synaptotagmin and SNAREs. Science *304*, 435–438.

Weber, T., Zemelman, B.V., McNew, J.A., Westermann, B., Gmachl, M., Parlati, F., Söllner, T.H., and Rothman, J.E. (1998). SNAREpins: minimal machinery for membrane fusion. Cell *92*, 759–772.

Weninger, K., Bowen, M.E., Chu, S., and Brunger, A.T. (2003). Single-molecule studies of SNARE complex assembly reveal parallel and antiparallel configurations. Proc. Natl. Acad. Sci. USA *100*, 14800–14805.

Woodbury, D.J., and Rognlien, K. (2000). The t-SNARE syntaxin is sufficient for spontaneous fusion of synaptic vesicles to planar membranes. Cell Biol. Int. *24*, 809–818.

Xiao, W., Poirier, M.A., Bennett, M.K., and Shin, Y.K. (2001). The neuronal t-SNARE complex is a parallel four-helix bundle. Nat. Struct. Biol. *8*, 308–311.

Xue, M., Reim, K., Chen, X., Chao, H.T., Deng, H., Rizo, J., Brose, N., and Rosenmund, C. (2007). Distinct domains of complexin I differentially regulate neurotransmitter release. Nat. Struct. Mol. Biol. *14*, 949–958.

Zhang, F., Chen, Y., Kweon, D.H., Kim, C.S., and Shin, Y.K. (2002). The four-helix bundle of the neuronal target membrane SNARE complex is neither disordered in the middle nor uncoiled at the C-terminal region. J. Biol. Chem. *277*, 24294–24298.

Zilly, F.E., Sorensen, J.B., Jahn, R., and Lang, T. (2006). Munc18-bound syntaxin readily forms SNARE complexes with synaptobrevin in native plasma membranes. PLoS Biol. *4*, e330.

Note Added in Proof

Recently, Rizo and coworkers have also found an interaction between the Munc13 MUN domain and membrane-anchored SNARE complexes. Guan, R., Dai, H., and Rizo, J. (2008). Binding of the Munc13-1 MUN domain to membrane-anchored SNARE complexes. Biochemistry, in press.

